

See discussions, stats, and author profiles for this publication at: <https://www.researchgate.net/publication/263980562>

# Unique Type II Halogen···Halogen Interactions in Pentafluorophenyl-Appended 2,2'-Bithiazoles

ARTICLE *in* CRYSTAL GROWTH & DESIGN · FEBRUARY 2013

Impact Factor: 4.89 · DOI: 10.1021/cg3012298

---

CITATIONS

18

---

READS

29

4 AUTHORS, INCLUDING:



Raja Siram

Weizmann Institute of Science

11 PUBLICATIONS 81 CITATIONS

SEE PROFILE

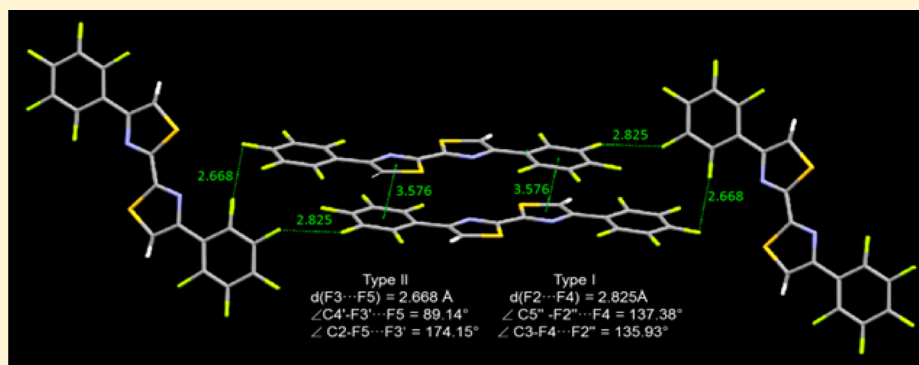
# Unique Type II Halogen...Halogen Interactions in Pentafluorophenyl-Appended 2,2'-Bithiazoles

Published as part of the *Crystal Growth & Design* virtual special issue in honor of Prof. G. R. Desiraju.

Raja Bhaskar Kanth Siram,<sup>‡</sup> Durga Prasad Karothu,<sup>‡</sup> Tayur N. Guru Row,<sup>\*</sup> and Satish Patil<sup>\*</sup>

Solid State and Structural Chemistry Unit, Indian Institute of Science, Bangalore 560012, India

## Supporting Information



**ABSTRACT:** Herein, we report the design and synthesis of 2,2'-bithiazole derivatives with efficient intermolecular halogen interactions. The single crystal X-ray diffraction studies revealed unique type-II halogen interactions in these derivatives. The shortest type-II  $F \cdots F$  interactions within the distance of 2.67 Å, at an angle of 89.1° and 174.2°, was observed for the first time. The Gaussian calculations were performed to further establish predominant  $F \cdots F$  interactions.

The burgeoning attention on fluorinated organic compounds has been important for the last 17 years, due to their applications in life science. From its early inception of fluorine as a vital element in drugs, there have been a large number of publications on fluorinated drugs.<sup>1</sup> However, not many applications of fluorinated compounds is seen in the domain of opto-electronics. In general, electron-withdrawing groups like fluorine, cyano, and nitro, etc. or electron donating substituents such as alkoxy, alkylamino, etc. can lower or raise the energies of the highest occupied molecular orbital (HOMO) and the lowest unoccupied molecular orbital (LUMO) relative to the unsubstituted system.<sup>2</sup> The redox and optical properties of the heterocyclic derivatives can be altered by the substitution of electron-donating or electron-withdrawing groups.<sup>3,4</sup> These modifications ultimately affect the physical and chemical properties of the resultant derivatives and define its role in various device configurations.<sup>5</sup>

Replacing hydrogen atoms by fluorine can profoundly vary the physical and chemical properties of compounds caused by its electronegativity, low polarizability, bond strength, and even the electron density distribution.<sup>6–8</sup> Because of these vivid properties, fluorine has an immense influence on inter- and intramolecular interactions.<sup>9</sup> Even though fluorine is a highly electronegative element, it forms difluorine rather than repelling another fluorine.<sup>10</sup> This leads to having prolonged snoop on the  $X-F \cdots F-X$  interaction until now. With dependance on the geometry of the halogen atoms, halogen–halogen

interactions are classified into two types, type I (cis and trans) with  $\theta_1 \approx \theta_2$  and type II with  $\theta_1 \approx 90^\circ$  and  $\theta_2 \approx 180^\circ$ , as depicted in Figure 1.<sup>11</sup> Type II interactions are formed through polarization of halogen atoms, whereas type I interactions are caused by close packing and do not form stabilizing interactions.<sup>1,11</sup> Over the years, type II interaction has grabbed more attention and have been further substantiated by several splash reports showing these halogen–halogen interactions.<sup>12</sup>

A CSD search (version 1.14, 2012) shows 5347 molecules containing  $X-F \cdots F-X$  (where X is any element) type I and type II interactions at distances ranging from 2.0 to 3.2 Å. Figure 2 depicts 614 hits of these, which show type II  $F \cdots F$  interactions where the angles were restricted to  $\theta_1 = 60–90^\circ$  and  $\theta_2 = 150–180^\circ$ . The number reduces to only 2 cases when the distance range is shortened to 2.6–2.7 Å. With a restriction of the angles to  $\theta_1 = 80–90^\circ$  and  $\theta_2 = 170–180^\circ$  in the CSD search, while keeping the distance range as 2.0–3.2 Å, 52 molecules are observed to show these interactions. Further shortening of the  $F \cdots F$  distance to 2.6–2.7 Å ( $\theta_1 = 80–90^\circ$  and  $\theta_2 = 170–180^\circ$ ) shows no hits. This has captivated our attention to synthesize fluorinated derivatives and exploiting shorter  $F \cdots F$  interactions within the proximate angle range. We have explored 2,2'-

Received: August 25, 2012

Revised: February 11, 2013

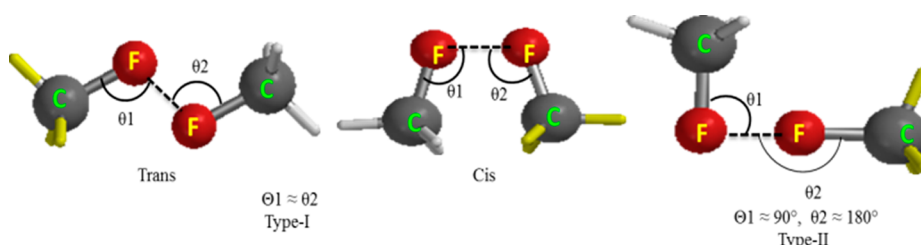


**Figure 1.** Graphical representation of type I (cis and trans) and type II F...F interactions.

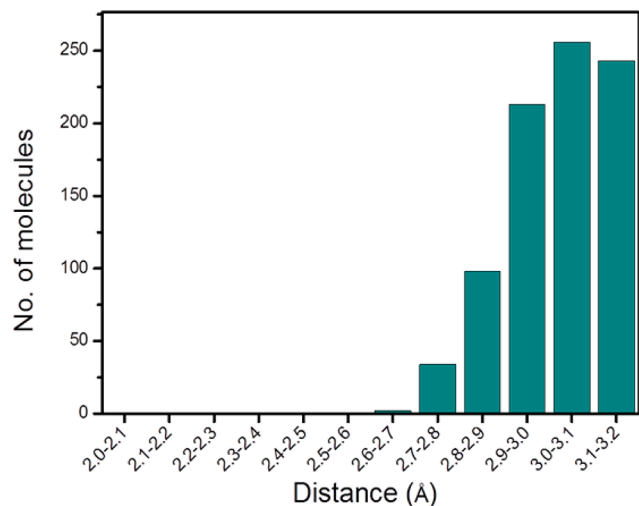


**Figure 2.** CSD search for number of molecules showing F...F interactions, where the angles  $\theta_1 = 60\text{--}90^\circ$  and  $\theta_2 = 150\text{--}180^\circ$ . Criteria: distances (2.0–3.2 Å, no ions, not disordered, only organics, and intermolecular contacts).

bithiazole-based derivatives to study the halogen...halogen interactions by substitution with pentafluorophenyl group.

2,2'-Bithiazoles are a very important class of heterocycles, in which an imine nitrogen is substituted in place of the carbon atom at the 3 position of thiophene, which facilitates the electron withdrawing nature to the five-membered ring, due to the high electron affinity of the nitrogen atom. These derivatives are widely used in a variety of applications which include organic light-emitting diodes, organic solar cells, and field-effect transistors.<sup>13–15</sup> We report, herein, synthesis of pentafluorophenyl appended bithiazole derivatives and high-

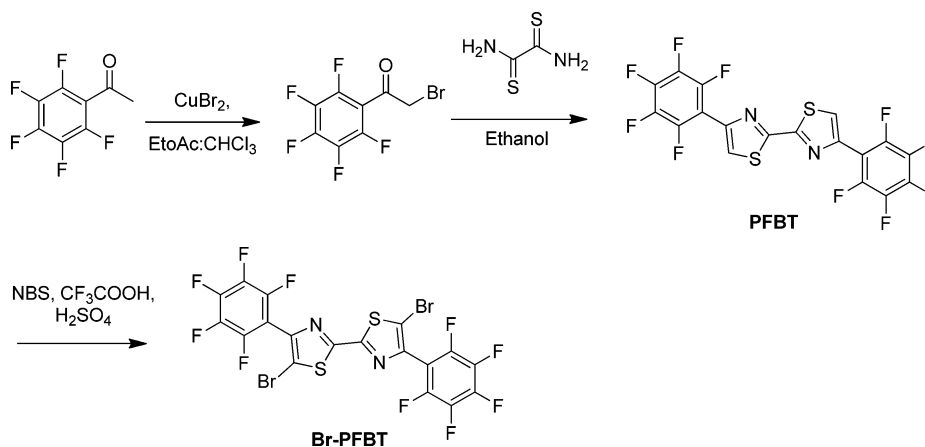
light the attenuated type II halogen–halogen (fluorine and bromine) short contacts by single crystal X-ray diffraction studies.

Scheme 1 illustrates the synthesis and molecular structure of the new bithiazole derivative, 4,4'-bis(perfluorophenyl)-2,2'-bithiazole (PFBT). PFBT was synthesized in high yield (83%) through the Hantzsch thiazole synthesis, by the condensation of 2-bromo-1-(perfluorophenyl) ethanone with dithioamide in ethanol under reflux conditions. After filtration of the solid, product was recrystallized by the slow evaporation of its saturated solution in ethanol. Our attempts of the dibromination of PFBT with standard brominating procedures like NBS in different solvents, AcOH, CHCl<sub>3</sub>, THF, or AcOH – CHCl<sub>3</sub> (1:1) and bromine gas in CHCl<sub>3</sub>, did not succeeded. Finally, our attempt at bromination under strong acidic solvent conditions, such as trifluoroacetic acid, provided the dibrominated product (Br-PFBT). All these derivatives are characterized by <sup>1</sup>H, <sup>19</sup>F, and <sup>13</sup>C NMR.

Single crystal X-ray diffraction data sets were collected on an Oxford Xcalibur (Mova) diffractometer equipped with an EOS CCD detector using MoK $\alpha$  radiation ( $\lambda = 0.71073$  Å).<sup>16</sup> The crystal was maintained at 110 K during data collection using the Oxford Instruments Cryojet-HT controller.<sup>17</sup> All structures were solved by direct methods using SHELXS-97 and refined against F<sup>2</sup> using SHELXL-97.<sup>18</sup> H atoms were located geometrically and refined isotropically. The WinGX package was used for refinement and production of data tables and ORTEP-3 for structure visualization and making the molecular representations.<sup>19,20</sup> Analysis of the H-bonded and  $\pi\cdots\pi$  interactions was carried out using PLATON for all the structures.<sup>21</sup> Packing diagrams were generated using MERCURY.<sup>22</sup>

The single crystals of compounds PFBT and Br-PFBT suitable for X-ray diffraction analyses were efficaciously

#### Scheme 1. Synthesis of Pentafluorophenyl-Appended Bithiazole Derivative



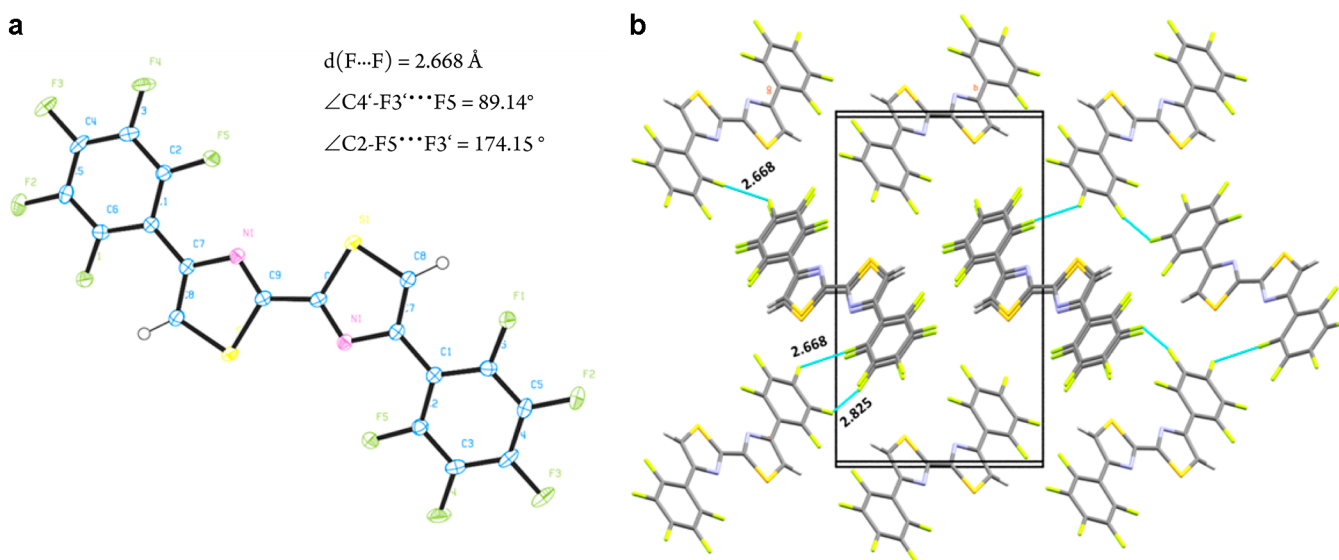


**Figure 3.** (a) ORTEP diagram of compound PFBT with displacement ellipsoids at a 50% probability level at 110 K. (b) Packing diagram of compound PFBT along the *a* axis showing type I and type II F...F contacts along with  $\pi\cdots\pi$  stacking.

obtained by slow evaporation of ethanol at ambient temperatures. Both compounds, PFBT and Br-PFBT, are exhibiting the type II halogen contacts (Table S2 of the Supporting Information). The compound PFBT<sup>23</sup> crystallizes in a monoclinic space group  $P2_1/n$  with  $Z = 2$  and  $Z'$  is 1/2. In crystal packing, molecules are arranged in herringbone packing along the *a* direction (Figure 3b). The packing shows habitual type I F...F contacts in between F4 and F2 of two adjacent molecules at a distance of 2.83 Å, where the angles are 137.4° and 135.9° for  $\angle C5''-F2''\cdots F4$  and  $\angle C3-F4\cdots F2''$ , respectively (Figure 3). The structure determined for PFBT exhibited the type II fluorine contacts at a short distance of 2.67 Å in between the F5 and F3 of the two adjacent molecules, where the angles are  $\theta_1 = 89.1^\circ$  and  $\theta_2 = 174.2^\circ$  for  $\angle C4'-F3'\cdots F5$  and  $\angle C2-F5\cdots F3'$ , respectively (Figure S1 of the Supporting Information). As mentioned earlier, the CSD search reveals only two molecules (distance: 2.6–2.7 Å, angles: 60–90° and 150–180°), where the first molecule confirms type II contact at a distance of 2.68 Å, in which the angles were 88.1° and 160.6°. The second molecule shows angles 87.7° and 163.4°, respectively, where the distance is 2.69 Å. Apart from having a shorter F...F contact, the PFBT molecule shows  $\pi\cdots\pi$  stacking between the thiazole rings and the phenyl rings. The distance between cg(1a) and cg(thiazole)(2b) is 3.58 Å, whereas the same remains for cg(1b') and cg(thiazole)(2a') (Figure S2 of the Supporting Information).

Seik Weng Ng has reported the structure of the phenyl derivative which shows no specific or significant interactions in the packing.<sup>26</sup> Substitution of hydrogen by fluorine provides evidence for strong intermolecular type II halogen–halogen interactions and  $\pi\cdots\pi$  stacking. This molecule demonstrates the type I and type II fluorine contacts which were depicted in Figure 3b.

The energies of monomer PFBT and its dimer were calculated using Gaussian09. Single crystal coordinates were used as input for calculations. These Gaussian calculations employed the split-valence double-exponential 6-31G++(d,p) basis sets with polarization functions.<sup>27</sup> DFT calculations in Gaussian09 were performed with Becke's three-parameter hybrid method,<sup>28</sup> combined with the nonlocal correlation

functional of Lee, Yang, and Parr<sup>29</sup> (B3LYP keyword in Gaussian09). Basis set superposition errors (BSSEs) were accounted for the counterpoise correction method.<sup>30</sup> From these calculations, it was found that the dimer interaction energy is 8.1 kJ/mol, confirming the attractive nature of the type II F...F interaction.

### HIRSHFELD SURFACE ANALYSIS

Further, the intermolecular contacts in the crystal structure of PFBT are quantified via the Hirshfeld surface analysis,<sup>31,32</sup> using the crystal explorer.<sup>33</sup> Through the Hirshfeld surface analysis, one can visualize the intermolecular interactions in crystal structures.<sup>34,35</sup> In the current study, the contacts involving F atoms and H...F are mainly estimated. The percentage of contributions to the Hirshfeld surface areas for these contacts and “other” (F...C, C...S, C...C, H...S, and N...C) intermolecular contacts are shown in Figure S3 of the Supporting Information. The analysis shows the F...F halogen contact as the dominating one (45.0%) in terms of Hirshfeld surface sharing, whereas only ~12% contribution comes from the H...F contacts. The C...F and C...C contacts both contribute ~30.0% to the Hirshfeld surface areas. However, it is notable that these percentage contributions do not distinguish between the close and distant contacts. The major contacts C–F...F–C halogen contacts are predominantly highlighted by conventional mapping of  $d_{\text{norm}}$  on molecular Hirshfeld surfaces (Figure 4). The dark red spots on the Hirshfeld surfaces indicate the F...F interaction.

Substitution of bromine in place of hydrogen atoms in PFBT leads the compound Br-PFBT<sup>36</sup> to crystallizes in a monoclinic space group  $P2_1/c$  with  $Z = 2$ , whereas  $Z' = 1/2$ . The hydrogen atoms in the compound PFBT are replaced by bromine atoms in this molecule, which shows significant variability from compound PFBT in packing. The molecules are arranged in a herringbone manner (Figure 5b), even though the size, electronegativity, and the repulsion between fluorine and bromine leads to the twisting of two pentafluorophenyl rings at a dihedral angle of 59.2°. This guided the packing of Br-PFBT to be different from that of compound PFBT. Prior to our attention, this compound also shows type II halogen–halogen

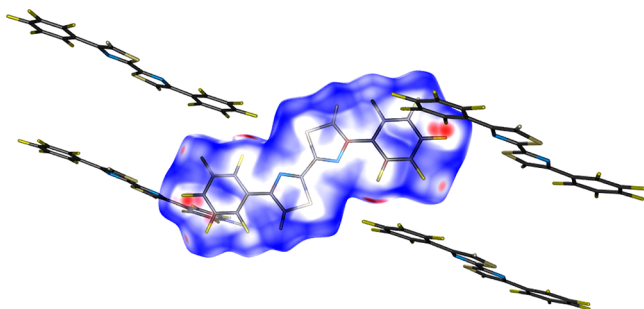


**Figure 4.**  $d_{\text{norm}}$  mapped on Hirshfeld surfaces for visualizing the F...F contacts.

interactions between bromine atoms at a distance of 3.68 Å, where the angles are 68.9° and 174.8° for  $\angle\text{C7}-\text{Br1}\cdots\text{Br1}'$  and  $\angle\text{C7}'-\text{Br1}'\cdots\text{Br1}$ , respectively (Figure S4 of the Supporting Information). Further stability is imparted by the S...F interactions at a distance of 3.20 Å.

In conclusion, the pentafluorophenyl appended 2,2'-bithiazole derivative was synthesized for the first time. The single crystal X-ray studies show the unusual strong type II F...F interactions, where  $\theta_1$  and  $\theta_2$  are proximate to 90° and 180°, respectively. PFBT also shows usual type I F...F interactions. From the Gaussian calculations, it is found that the interaction between both fluorine atoms is attractive and Hirshfeld surfaces confirm that the F...F contacts are predominant. Upon bromination, the type II Br...Br interaction was observed and the packing was further stabilized by the S...Br interactions. Charge density studies of these type II interactions and device fabrication is an ongoing work in our laboratory. Further work will focus on the extension of the conjugation with different aromatic and heteroaromatic substituents.

## ■ ASSOCIATED CONTENT

### Supporting Information

Experimental procedures regarding synthesis and NMR spectra of the derivatives, packing diagrams, and the full crystallographic details of the derivatives. This material is available free of charge via the Internet at <http://pubs.acs.org>.

## ■ AUTHOR INFORMATION

### Corresponding Author

\*E-mail: [satish@sscu.iisc.ernet.in](mailto:satish@sscu.iisc.ernet.in) and [ssctng@sscu.iisc.ernet.in](mailto:ssctng@sscu.iisc.ernet.in).

### Author Contributions

‡These authors contributed equally.

### Notes

The authors declare no competing financial interest.

## ■ ACKNOWLEDGMENTS

S.P. thanks ISRO for supporting this work through the project ISTC/CSS/STP/252 and S.R.B.K. and D.P.K. thank CSIR for the Senior Research Fellowship. T.N.G. thanks the DST, New Delhi for the J. C. Bose Fellowship.

## ■ REFERENCES

- (1) Reichenbacher, K.; Suss, H. I.; Hulliger, J. *Chem. Soc. Rev.* **2005**, 34, 22.
- (2) Casado, J.; Pappenfus, T. M.; Miller, L. L.; Mann, K. R.; Ortí, E.; Viruela, P. M.; Pou-AméRigo, R.; Hernández, V.; López Navarrete, J. T. *J. Am. Chem. Soc.* **2003**, 125, 2524.
- (3) Casado, J.; Miller, L. L.; Mann, K. R.; Pappenfus, T. M.; Higuchi, H.; Ortí, E.; Milián, B.; Pou-AméRigo, R.; Hernández, V.; López Navarrete, J. T. *J. Am. Chem. Soc.* **2002**, 124, 12380.
- (4) Brédas, J.-L. *Adv. Mater.* **1995**, 7, 263.
- (5) Facchetti, A.; Yoon, M.-H.; Stern, C. L.; Hutchison, G. R.; Ratner, M. A.; Marks, T. J. *J. Am. Chem. Soc.* **2004**, 126, 13480.
- (6) Chopra, D.; Cameron, T. S.; Ferrara, J. D.; Guru Row, T. N. *J. Phys. Chem. A* **2006**, 110, 10465.
- (7) Chopra, D.; Row, T. N. G. *CrystEngComm* **2011**, 13, 2175.
- (8) Berger, R.; Resnati, G.; Metrangola, P.; Weber, E.; Hulliger, J. *Chem. Soc. Rev.* **2011**, 40, 3496.

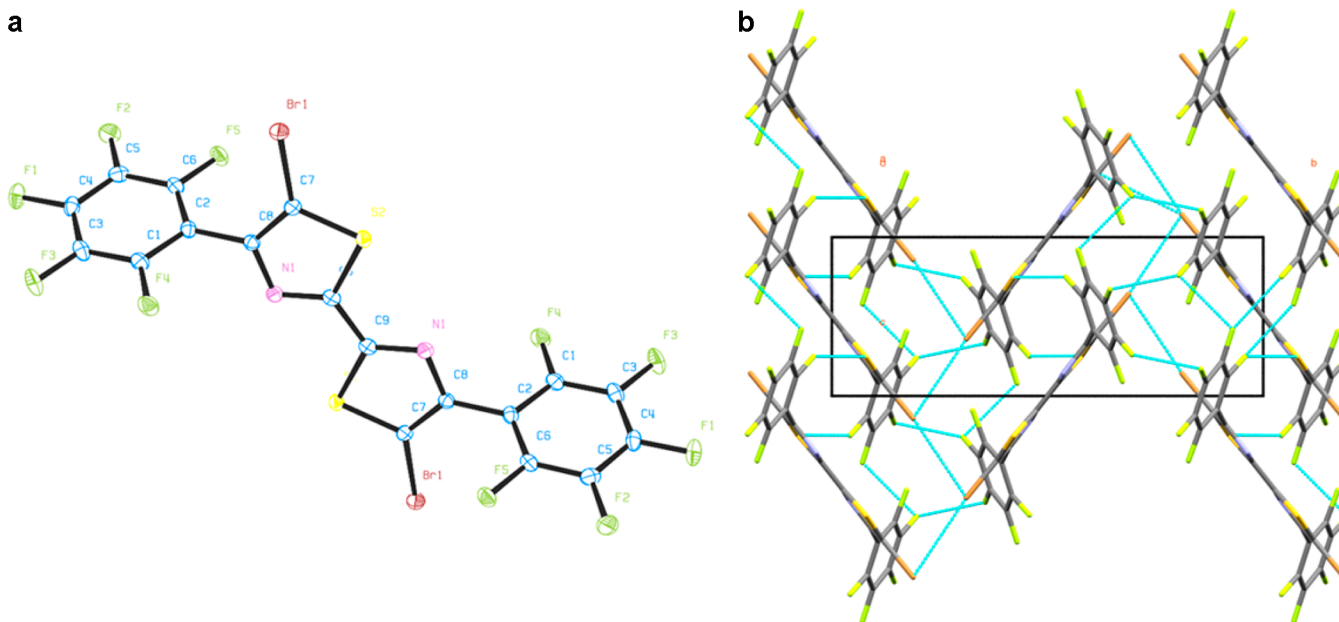


**Figure 5.** (a) ORTEP diagram of compound Br-PFBT, with displacement ellipsoids at the 50% probability level at 110 K. (b) Packing diagram of compound Br-PFBT along the *a* axis showing type I and type II contacts and S...F contacts.



- (9) Chopra, D.; Guru Row, T. N. *CrystEngComm* **2008**, *10*, 54.
- (10) Chopra, D. *Cryst. Growth Des.* **2012**, *12*, 541.
- (11) Ramasubbu, N.; Parthasarathy, R.; Murray-Rust, P. *J. Am. Chem. Soc.* **1986**, *108*, 4308.
- (12) Dikundwar, A. G.; Row, T. N. G. *Cryst. Growth Des.* **2012**, *12*, 1713.
- (13) Lin, Y.; Fan, H.; Li, Y.; Zhan, X. *Adv. Mater.* **2012**, *24*, 3087.
- (14) Ando, S.; Murakami, R.; Nishida, J.-i.; Tada, H.; Inoue, Y.; Tokito, S.; Yamashita, Y. *J. Am. Chem. Soc.* **2005**, *127*, 14996.
- (15) MacLean, B. J.; Pickup, P. G. *J. Mater. Chem.* **2001**, *11*, 1357.
- (16) Oxford Diffraction CrysAlis PRO CCD and CrysAlis PRO RED, Oxford Diffraction Ltd: Yarnton, England, 2009.
- (17) Oxford Instruments, Cryojet XL/HT controller; Oxford Diffraction Ltd: Yarnton, England, 2009.
- (18) Sheldrick, G. M. *Acta Crystallogr., Sect. A: Found Crystallogr.* **2008**, *64*, 112.
- (19) Farrugia, L. J. *J. Appl. Crystallogr.* **1999**, *32*, 837.
- (20) Farrugia, L. J. *J. Appl. Crystallogr.* **1997**, *30*, 565.
- (21) Spek, A. J. *J. Appl. Crystallogr.* **2003**, *36*, 7.
- (22) Macrae, C. F.; Edgington, P. R.; McCabe, P.; Pidcock, E.; Shields, G. P.; Taylor, R.; Towler, M.; Streek, J. *J. Appl. Crystallogr.* **2006**, *39*, 453.
- (23) Crystal data for PFBT: CCDC no. 889643; molecular formula:  $C_{18}H_{10}F_{10}N_2S_2$ ; monoclinic;  $a = 4.9358(3)$  Å;  $b = 9.9438(5)$  Å;  $c = 16.7977(8)$  Å;  $\beta = 90.352(5)^\circ$ ;  $V = 824.43(8)$  Å<sup>3</sup>;  $T = 120(1)$  K; space group,  $P2_1/n$ ,  $Z = 2$ .
- (24) Ning, Y.; Zhu, H.; Chen, E. Y. X. *J. Organomet. Chem.* **2007**, *692*, 4535.
- (25) Tamm, N. B.; Sidorov, L. N.; Kemnitz, E.; Troyanov, S. I. *Chem.–Eur. J.* **2009**, *15*, 10486.
- (26) Ng, S. *Acta Crystallogr., Sect. E: Struct. Rep. Online* **2010**, *66*, o2030.
- (27) Hariharan, P. C.; Pople, J. A. *Theor. Chim. Acta* **1973**, *28*, 213.
- (28) Becke, A. D. *J. Chem. Phys.* **1993**, *98*, 5648.
- (29) Lee, C.; Yang, W.; Parr, R. G. *Phys. Rev. B: Condens. Matter Mater. Phys.* **1988**, *37*, 785.
- (30) Boys, S. F.; Bernardi, F. *Mol. Phys.* **1970**, *19*, 553.
- (31) Spackman, M. A.; McKinnon, J. J. *CrystEngComm* **2002**, *4*, 378.
- (32) McKinnon, J. J.; Spackman, M. A.; Mitchell, A. S. *Acta Crystallogr., Sect. B: Struct. Sci.* **2004**, *60*, 627.
- (33) (a) Wolff, S. K.; Grimwood, D. J.; McKinnon, J. J.; Turner, M. J.; Jayatilaka, D.; Spackman, M. A., *CrystalExplorer 2.0 (Version 3.0)*; University of Western Australia: Perth, Australia, 2012. (b) Spackman, M. A.; Jayatilaka, D. *CrystEngComm* **2009**, *11*, 19–32.
- (34) Munshi, P.; Skelton, B. W.; McKinnon, J. J.; Spackman, M. A. *CrystEngComm* **2008**, *10*, 197.
- (35) McKinnon, J. J.; Jayatilaka, D.; Spackman, M. A. *Chem. Commun.* **2007**, 3814.
- (36) Crystal data for Br-PFBT: CCDC no. 889644; molecular formula:  $C_{18}Br_2F_{10}N_2S_2$ ; monoclinic;  $a = 9.9430(5)$  Å;  $b = 15.7223(7)$  Å;  $c = 6.2495(3)$  Å;  $\beta = 101.142(2)^\circ$ ;  $V = 958.55(4)$  Å<sup>3</sup>;  $T = 120(1)$  K; space group,  $P2_1/c$ ,  $Z = 2$ .